heritage

MDPI

Article

Mortar Characterization and Radiocarbon Dating as Support for the Restoration Work of the Abbey of *Santa Maria di Cerrate* (Lecce, South Italy)

Giovanna Vasco, Antonio Serra, Giovanni Buccolieri, Daniela Manno, Lucio Calcagnile, Gianluca Quarta and Alessandro Buccolieri *

Center of Applied Physics, Dating and Diagnostics (CEDAD), Dipartimento di Matematica e Fisica "Ennio De Giorgi", University of Salento, 73100 Lecce, Italy
* Correspondence: alessandro.buccolieri@unisalento.it

Abstract: During the restoration work promoted by the FAI foundation (*Fondo Ambiente Italiano*) of the abbey of *Santa Maria di Cerrate* (Lecce, Apulia, South Italy), multidisciplinary analyses have been realized to support conservators and art historians for the safeguard and valorization of the most important byzantine evidence (12th–13th century) in Apulia. In this paper, mortar samples have been investigated using scanning electron microscopy (SEM-EDX) and X-ray diffraction (XRD) to characterize the observed materials, directing conservators for the integration interventions with compatible realizations. Moreover, the samples were compared with specimens taken from local quarries and the nearest coastline area, and vegetal fibers, embedded into the mortars were analyzed by applying radiocarbon dating by accelerator mass spectrometry (AMS). It was thus possible to give a contribution to the historical-artistic research related to the building techniques, the ratio aggregates/binder and the employed materials of the mortars and the dating of the mural paintings between the end of the 12th century and the first half of the 13th century.

Keywords: medieval mortars; *Santa Maria di Cerrate*; SEM-EDX; XRD; radiocarbon dating

Citation: Vasco, G.; Serra, A.; Buccolieri, G.; Manno, D.; Calcagnile, L.; Quarta, G.; Buccolieri, A. Mortar Characterization and Radiocarbon Dating as Support for the Restoration Work of the Abbey of *Santa Maria di Cerrate* (Lecce, South Italy). *Heritage* **2022**, *5*, 4161–4173. https://doi.org/10.3390/heritage5040215

Academic Editors: Daniela Fico and Daniela Rizzo

Received: 24 November 2022
Accepted: 12 December 2022
Published: 15 December 2022

1. Introduction

The monastery of *Santa Maria di Cerrate* (Lecce, Apulia, South Italy) is a complex of structures (12th–20th century) due to several uses of the area that modified it over time (Figure 1). In fact, the Italian-Greek community of monks that founded the monastery was gradually replaced by the organization of a typical Southern Italian farm.

The conservation activities for its redevelopment offered an interesting meeting point between diagnostic and historical studies, together with the stylistic knowledge correlated to the context. In fact, scientific methodologies of investigation have been applied to characterize the frescos of the abbey and their degradation state to support the conservation treatments. This opportunity was also seized to nail their chronology down and to relate the materials with the employed artistic techniques.

In agreement with the Superintendence of Cultural Heritage and the conservation director of the FAI (Fondo Ambiente Italiano) foundation, through multidisciplinary collaboration with conservators, some specimens were sampled, trying to limit as much as possible the invasiveness of the sampling and considering the required instrumental quantities.

For conservators, it was particularly necessary to identify the original pigments used for the frescos to properly clean their surface and to characterize the degradation of the bleached areas. Moreover, the composition of the mortars inside the church and their binder/aggregates ratio were required to replenish the gaps of renders and plaster layers using materials with suitable physicochemical properties.

(**a**) (**b**)

Figure 1. External (**a**) and internal (**b**) photos of the abbey of *Santa Maria di Cerrate*.

The characterization of the frescoes regarding their conservation state and the results of the pigment analysis was reported in previous work [1]. In particular, the bleaching alterations were related to the photocatalytic effect of titanium dioxide, which was found together with chromium, attributable to previous documented restorations (1960s). About the pigments, in addition to the common presence of hematite and goethite for the landscapes and the characters, the rare use of the expensive lapis lazuli blue with carbon black was identified in the background of the wall paintings. Finally, for historical-artistic research, it was possible to define the *mezzo fresco* technique through morphological and qualitative analyses on a cross-section.

Regarding the building techniques, petrographic, mineralogical and chemical characteristics of the mortars were investigated during previous conservation work, concerning the external walls of the church, the sculptured portico and the buildings around the courtyard [2]. This study highlighted the differences between medieval mortars, based on carbonate aggregate, and post-medieval mortars with mostly siliciclastic aggregate.

Moreover, to complete the restoration work, it was still necessary to characterize the mortars inside the church in the points required by conservators to finish the integrations. Therefore, in this study, we report the granulometric and mineralogical analyses performed on the samples from the mortars inside the church, which also gave the opportunity to contribute to the dating of the frescoes with scientific methods.

1.1. The Abbey of Santa Maria di Cerrate

Between the 9th and the 11th century, Apulia was a byzantine region, culturally influenced by the presence of political and ecclesiastical officials coming from different areas of the Empire, followed by Greek artists. The artistic production was thus the distinctive result of a combination of Greek conservative features and updated byzantine art trends of monumental painting, grafted into local specificities thanks to the cultural absorption by local inhabitants. Therefore, after the end of the byzantine domination because of the Norman conquest, the byzantine language partially survived, above all in the area known as Terra d'Otranto where entrenched connections were established with Greece, Cappadocia, Syria, Egypt, Cyprus and Corfu, thanks to its geographical position that made it a crossroad for pilgrims and trades.

During the 12th century, where the Apulian Romanesque architecture and sculpture reached their apex, the Apulian-byzantine wall paintings have gradually gone and disappeared. However, byzantine paintings survived until the 14th century in the Salento peninsula, where Italian-Greek communities existed until the 17th century, creating a continuous dialectic between western and eastern cultures in a kaleidoscopic society [3].

Therefore, the church of *Santa Maria di Cerrate* (14 km north of Lecce, South Italy), stands out as one of the few and most important evidences of monumental byzantine

painting of the 12th–13th century in a unique framework of the architectural and sculptural Apulian Romanesque style [4]. In addition to the church (12th century), the complex consists of a carved portico (13th century), Baroque additions (16th–17th century) realized during the restoration work by the Roman curia after the Basilian monks left in the 14th century, and buildings (18th–20th century) dedicated to stalls, granaries and underground mills for cereal production and lamp oil-making developed after Turkish pirate raids [5–10]. These different phases led to several modifications of the wall paintings, which were updated in between the 14th and the 15th century and whitewashed when the complex was completely abandoned by the Church, becoming exclusively a farm.

From 1965 AD, the Province of Lecce opened the Museum of Arts and Folklore of Salento, also promoting the architectural restoration (up to the 1970s) of the complex by the architect Franco Minissi [10,11]. In the same period (1975 AD), the Central Institute for Restoration of Rome (ICR) restored the whitewashed frescoes and detached those of the 14th–15th century, discovering the original wall paintings (12th–13th century) in the underlying layer [10,11].

Finally, in 2012 AD, the abbey was entrusted to the FAI foundation for thirty years, becoming its first Apulian beneficiary, with the purpose of making it a cultural center.

1.2. The Wall Paintings of Santa Maria di Cerrate

Regarding the different phases of the frescoes, those in the apses are the oldest, stylistically dated at the end of the 12th century [3,4,12]. In the central apse, the *Ascension* is represented according to pure byzantine canons, without any contamination of the *Maiestas Domini* [3,4,12]. In fact, the whole arrangement of the apse shows a common imprint with specific references to Macedonia and in particular to Kurbinovo, Kastoria, Nerezi, Skopje and Thessalonica [3,4,12]. The images are framed by vegetal motifs and a decoration with white pseudo-Kufic letters on a blue background, as a reference to the Egyptian Coptic churches, built under the Fatimids [3,4,12]. In the lower part of the central apse, five bishop saints were painted, including Saint John Chrysostom.

The sequence of bishops continues in the right apse, under the representation of Saint John the Baptist, while the wall paintings of the left apse have been lost. Monks and deacons are represented in the arches with old repaints probably realized during the conservation treatments of the 17th century [3,4,12].

In the aisles, a series of monks, martyrs, bishops, hymnographer saints and knights were painted [3,4,12]. In particular, in the right aisle, the presence of the Virgin child between Saint Anne and Saint Joachim is recognizable, although part of the masonry collapsed. This event led to a casual reconstruction with the same stone bricks, without relocating them in the exact position according to the fresco representation.

On the counter-façade, the *koimesis* was realized together with holy figures.

All these frescoes have been considered contemporary with the realization of the ciborium which has a Greek inscription dated 1269 AD [3,4,12]. The only exception is the portion framed by the baroque altar of Saint Oronzo (right aisle), dated around the 14th century [3,4,12].

Regarding the detached frescoes located by ICR in the Museum of Arts and Folklore, both the *Death of the Virgin* (14th century), the *Annunciation*, the *Archangel Gabriel*, *Saint George rescuing the princess from the dragon* and the *Conversion of Saint Eustace* (15th century) are marked by a complex scenario with architectural structures and decorated clothes of the characters [12]. The authors are not known, but in the *Death of the Virgin*, a praying character defined by an inscription as "*The Pilgrim of Morciano*" was considered the commissioner of this wall painting [12].

2. Materials and Methods

2.1. Research Aims

In this study, the composition of the mortars inside the church and their binder/aggregates ratio were required by conservators to replenish the gaps at the level of renders and plaster

layers using materials with suitable physicochemical properties. Therefore, some samples from the required parts were analyzed using scanning electron microscopy (SEM-EDX) and X-ray diffraction (XRD), also testing a new method of image elaboration of macro and micro images for statistical analysis of particles [13].

In fact, historic mortars are composite materials with different compositions, depending on their typology (i.e., areal, hydraulic or mixed mortar), the ratio between their components (sand, lime, water, organic and inorganic additives), the production processes (with different kinetics of the carbonation mechanism during setting, hardening and ageing) and the material sources, also having differences in the mortar technologies in relation to the historical period [14–16]. Consequently, in conservation, materials with compatible physicochemical characteristics are necessary to prevent internal disconnections and tensions given by a different material reaction to external stresses and to environmental factors [17,18].

Moreover, the presence of different quarries (located next to the towns of Monteroni and Surbo) and the mouth of the Idume (Frigole) river close to the area of the abbey were considered as possible sources of the raw materials. Therefore, some reference samples were taken to compare the results of the mortars.

While sampling in the abbey, it was also possible to take vegetal remains embedded into the mortars and the plasters coming from the gaps to date the frescos on the walls of the aisles with radiocarbon dating using accelerator mass spectrometry (AMS) [19–21], thus giving art historians new information about the development of the building.

2.2. Sample Selection

For this study, five specimens were taken from the abbey. The sampling areas have been set out in Figures 2 and 3. The sampling areas were chosen by conservators together with the Superintendence, in the most representative parts of the aisles. In fact, differently from the apses, these areas needed strong conservative interventions and more information for their reconstruction. The most extended gaps were selected to avoid invasive sampling and new possible losses.

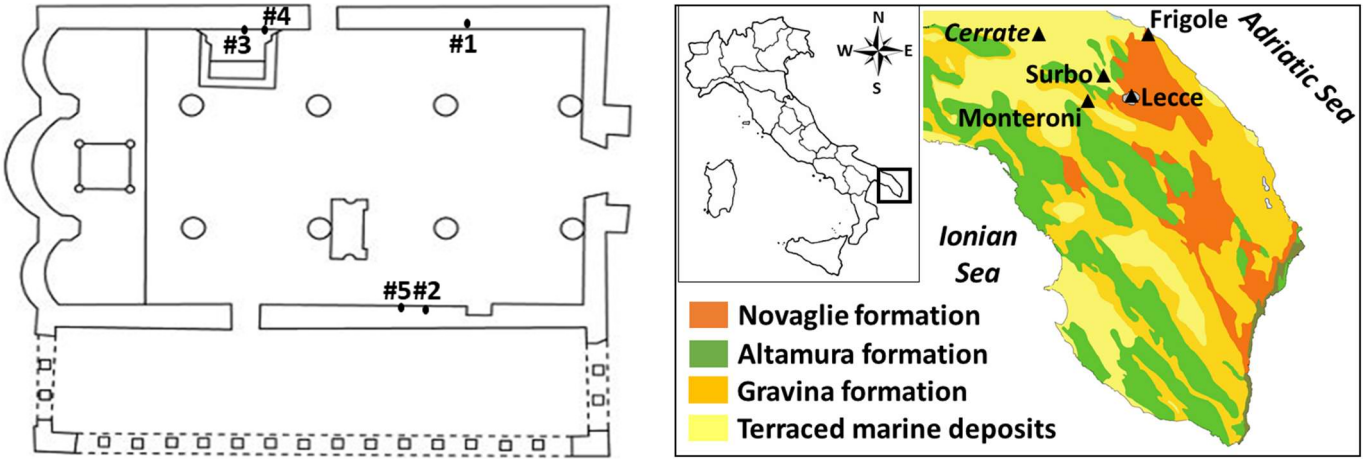

(**a**) (**b**)

Figure 2. Planimetry and measuring points in the abbey of *Santa Maria di Cerrate*: (**a**) Sampling area and geological characteristics of the area near Cerrate (**b**) showing the formations of Novaglie (bioconstructed calcarenites and brecce and limestones—Late Miocene), Altamura (laminated bioclastic micritic and calcarenitic limestone, with banks of dolomicritic parts with biostromal and rudist shells—Late Cretaceous), Gravina (biolimestone and biocalcirudites in intercalated banks with rare calcilutites—Lower Pleistocene) and Terrace marine deposits (Terraced Marine Deposits: sands, conglomerates, loam—Middle-Upper Pleistocene).

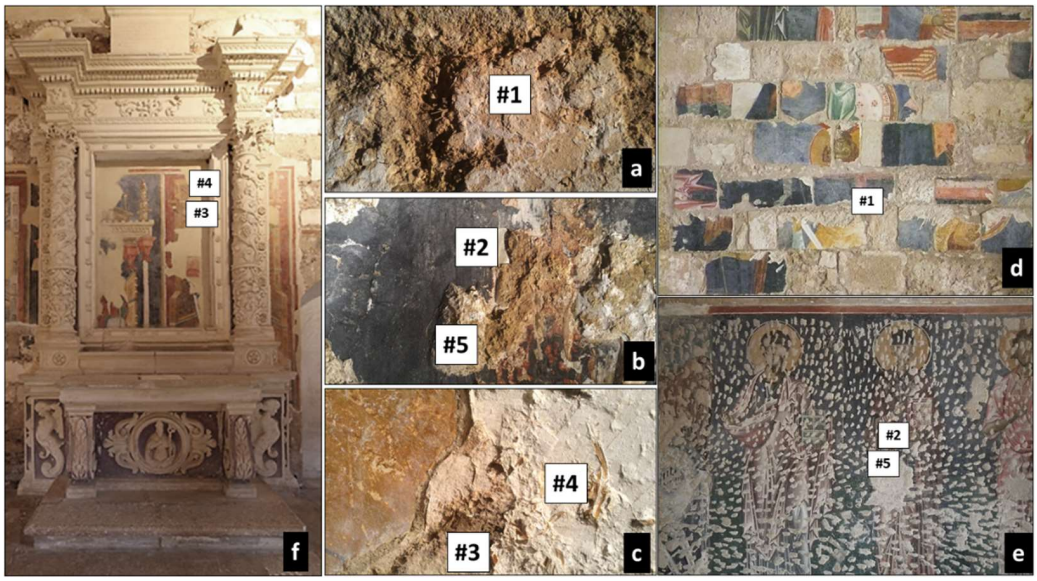

Figure 3. Sampling areas (**a**–**f**) inside the abbey of *Santa Maria di Cerrate*.

Three samples of mortars were taken from the aisles (Samples #1, #2 and #3), together with two samples of vegetal remains (Samples #4 and #5). Among the mortar samples, two of them were collected from the render layer and the last one from the plaster layer belonging to the frescoes. In particular, Sample #1 was collected as a compact material, while Samples #2 and #3 crushed during the sampling phase. Therefore, image elaboration of macro and micro images were repeated on Sample #1, completely crushing it to compare the method of particles' statistical analysis. In this second step, all material of the crushed Sample #1 was used, thus leading to a large area of analysis.

Regarding the vegetal remains, they were found coming out from the *arriccio* and render layers of the frescoes in the gaps.

Moreover, two rock samples were taken from the nearby quarries of Monteroni (Sample #6) and Surbo (Sample #7), while one sand sample (Sample #8) was collected in the coastline area of Frigole, from the mouth of the river Idume, just a few kilometers from the abbey. The quarries and the mouth were chosen because they were considered the most probable source of the employed raw materials due to their geographical proximity to the abbey. All the examined samples are listed in Table 1.

Table 1. Description of the analyzed samples.

Sample	Typology	Description
#1	Mortars	Render layer near the collapsed masonry of the right aisle
#2		Render layer of the left aisle
#3		Plaster layer next to the 14th-century fresco of the right aisle
#4	Vegetal remains	Vegetal remains from the *arriccio* next to the Sample #3
#5		Vegetal remains and one wooden fragment from the left aisle
#6	Rocks	Quarry of Monteroni—limestone
#7		Quarry of Surbo—limestone
#8	Sand	Coastline area of Frigole (river Idume)—sandstone

2.3. Scanning Electron Microscopy (SEM-EDX)

All micro images were acquired by scanning electron microscope JEOL model JSM-5410 LV with an emission source of tungsten filament, a resolution of 3.5 nm, a magnification of 100–200,000× and an acceleration voltage of 0.5–30 kV. The opportunity to perform investigations in low vacuum allowed to avoid charge accumulation for samples with

insulating properties without the need for a conductive coating. Analysis was processed using Link Isis software by Oxford Instruments and Image Pro-Plus by Media Cybernetics. For each sample, more than fifty images were taken, together with the characteristic X-ray spectra. The topographic distribution of the detected elements was acquired through elemental maps.

The digital processing of macro and micro images, taken respectively with the camera Nikon D80 and the scanning electron microscope, was carried out with ImageJ software, based on Sun-Java and developed by the National Institutes of Health [22]. The images, converted into 8-bit grayscale, were segmented into a new black-and-white figure using the threshold function, highlighting the components by assigning a defined threshold value to the pixel depending on their brightness. Using the analysis functions, images were processed and the components were converted into elliptical shapes. By associating the number of pixels with the dimensional reference value, it was possible to obtain the object dimensions. The area of the aggregates was thus estimated, identifying their volume ratio with the binder.

2.4. Structural Analysis

A diffractometer Rigaku model Miniflex was used for X-ray diffraction (XRD) analysis, employing Cu Kα radiation at 30 kV and 100 mA operating in step-scan mode from 10° to 80°, with a 0.020° step and a scan speed of 0.25 °·min^{-1}.

2.5. Radiocarbon Dating with AMS

After a careful selection carried out at the microscope Nikon SMZ 1500 in order to select the organic remains less affected by the degradation due to carbonation, the weight of the specimens was re-measured and a new lab code was assigned to each sample. In fact, the carbonation process involved in the hardening and setting phases of the frescoes consumes and degrades the vegetal materials, which could not survive the chemical treatments for radiocarbon dating.

Samples were treated by following the standard acid-alkali-acid procedure used at CEDAD [23]. For the first step, used to remove possible microscopic traces of carbonates and fulvic acids, 10 mL of 1% HCl solution were added. After reaching a pH value below 1, samples were washed with ultrapure deionized water until a pH higher than 5 was obtained. Humic acids were then removed with the second step, with 10 mL of 1% NaOH solution, followed by warm washings with ultrapure deionized water until reaching a pH below 9. The third step with 10 mL of 1% HCl solution was performed to remove the possible CO_2 dissolved during the previous treatment, until reaching a pH higher than 5. The extracted material was then combusted to carbon dioxide together with silver wool and copper oxide in quartz tubes flame-sealed under vacuum. The CO_2 was then cryogenically purified and transferred to the graphitization lines to be converted at 600 °C to graphite using hydrogen as the reducing agent and iron powder as the catalyst. The measurements of the radiocarbon content were carried out at the ^{14}C AMS beamline at CEDAD using a 3 MV HVEE Tandetron accelerator. The measured $^{14}C/^{12}C$ isotopic ratios were corrected for machine and processing background and isotopic fractionation by using the $\delta^{13}C$ term measured online with the AMS system. The measurement uncertainty was conservatively estimated as the larger between the ^{14}C counting statistic error and the data scattering of the ten measurements repeated for each sample. Saccharose C6 provided by the IAEA and oxalic acid II supplied by NIST (National Institute of Standards and Technology) were used as standard reference materials.

3. Results and Discussion

3.1. Granulometric Studies

All macro images and the images acquired through the SEM-EDX showed the presence of ground aggregates with elliptical and subspherical shapes immersed in a particularly fine particle size component. The presence of some micro cracks was probably related to

the shrinkage phenomenon during the carbonation reaction in the setting and hardening phase of the mortar. Moreover, a few lime lumps were observed only in Sample #2, with the rare presence of small granules, thus denoting a generally remarkable making process, with a good setting, hardening and ageing [14,24]. Furthermore, in all samples, the presence of vegetal remains was observed, used as reinforcing materials in agreement with the typical byzantine building technique [24–26], while no traces of fossils were found, despite being expected due to the known characteristics of the local limestone and sand [27].

Along with the abovementioned common features, important granulometric differences were identified together with the chemical characterization of the mortar components.

The digital processing of macro photographs allowed the investigation of the dimensional characteristics of the macro aggregates, while images acquired by SEM-EDX were used to investigate the micro components. Through the data obtained for macro photography, it was possible to estimate the percentage of aggregate and its volume ratio with respect to the binder.

Considering that among the three samples just Sample #1 remained fully compact, two processes were followed to test an explorative strategy for the granulometric test of imaging analysis for historical mortars: Sample #2 and Sample #3 were completely arranged on two different glass slides with proper tape in order to have all the forming particles laid on the same plane, while Sample #1 was first analyzed as a block.

Then the analysis was repeated unravelling Sample #1 it on a glass slide to check both the ratio between aggregates and binders was compatible, considering the aggregates are casually located in the matrix and their disposition was statistically representative even applying imaging analysis.

The steps of the digital imaging process of elaboration using ImageJ, given in 2.3 scanning electron microscopy (SEM-EDX), are illustrated in Figure 4 with the application on Sample #1. In particular, since the aggregates had mainly a subspherical shape, their dimensions were calculated using the diameter of Feret [13], defined as the mean value of a series of measures of the distance between two parallel tangents to the perimeter of the projected area from the particle, assumed to be hypothetical spherical.

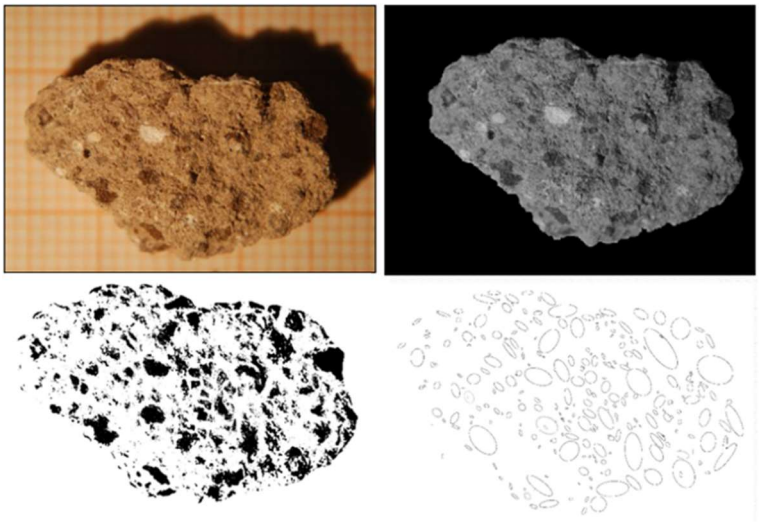

Figure 4. Digital elaboration of a macro photograph of Sample #1.

Throughout the macro images analysis, it was possible to estimate the areas covered by the aggregates and to verify the differences in the ratio between aggregates and binders (Table 2). In particular, the values found for Sample #1 (1:3) and Sample #2 (1:4) were in agreement with the historical byzantine practices [15,28–30], used both to reinforce the mortars and to slow down the carbonation process, thus giving more time to the artists to use the pigments for the fresco technique. Moreover, the considerable difference in the aggregates/binder ratio for Sample #3 (1:13) depended on the sampling realized on the

outer layer within the plaster, which commonly have a low content of aggregates with respect to the internal layers of the mortars. The elaboration on the crushed Sample #1 gave comparable results, confirming the volume aggregates/binder ratio (1:3).

Table 2. Percentage of aggregates in the binder and the volume aggregates to binder ratio.

Sample	Total Area of the Sample (mm^2)	Total Area of the Aggregates (mm^2)	Aggregates (%)	Aggregates/Binder Ratio
#1 (compact)	235	80.94	34.4	1:3
#1 (crushed)	1967	640.7	32.6	1:3
#2	204	52.75	25.8	1:4
#3	198	15.02	7.6	1:13

Micro images using SEM-EDX were used to investigate the differences among their micro components. In particular, the aggregates were identified with help of the X-ray microanalysis. Then, the morphological information obtained from SE images was obtained by applying the previously described imaging method of statistical analysis for particles. The results were given according to the Wentworth scale. Regarding their granulometric distribution, as shown in Table 3, Sample #1 was characterized by the higher granulometric dispersion, with a considerable presence of clay particles (80.20%) and silt (19.70%) with the smallest amount of sand whose diameter ranges from medium to very fine grains (0.10% in total). Sample #2 was quite homogeneous, but coarser than the previous one, with the presence of the smallest components classifiable in the silt category (95.69%) and with a higher amount of sand (4.31% in total) than Sample #1 also including a few coarse grains (0.01 %). Sample #3 resulted to have a rather thin granulometry mostly consisting of silt components (98.00%) and a small amount of aggregate ranging from medium to very fine sand (2% in total).

Table 3. Percentage of micro components of aggregates in the binders.

Sample	Granulometry (μm)	Number of Particles Based on the Diameter of Feret (μm)	Total Percentage (%)
#1	Clay particle (<3.9)	936.67	80.20
	Silt (3.9–62.5)	230.13	19.70
	Very fine sand grain (62.5–125)	0.93	0.07
	Fine sand grain (125–250)	0.2	0.02
	Medium sand (250–500)	0.07	0.01
	Coarse sand (500–1000)	0	0
#2	Clay particle (<3.9)	0	0
	Silt (3.9–62.5)	1079.67	95.69
	Very fine sand grain (62.5–125)	37.6	3.33
	Fine sand grain (125–250)	9.3	0.83
	Medium sand (250–500)	1.53	0.14
	Coarse sand (500–1000)	0.13	0.01
#3	Clay particle (<3.9)	0	0
	Silt (3.9–62.5)	829.87	98.00
	Very fine sand grain (62.5–125)	10.37	1.23
	Fine sand grain (125–250)	6.25	0.74
	Medium sand (250–500)	0.25	0.03
	Coarse sand (500–1000)	0	0

Regarding the X-ray microanalysis, the maps showed the widespread aggregates of different granulometry consisting of silica immersed in a matrix with very high calcium content and a general, but not so relevant, presence of iron for Sample #1 and Sample #2. Sample #3 was characterized by higher content of calcium and a considerable low

amount of aggregates and iron in accordance with its plaster function. The recorded X-ray spectra allowed the revelation of a very similar qualitative composition for all samples, which were further investigated realizing a relative percentage analysis of the main elements of the three samples. The analysis was performed with the ZAF correction for the matrix effects due to the atomic number of the elements, the phenomenon of absorption and the secondary fluorescence. The normalized concentrations of the major elements, conventionally expressed as %wt, are reported in Table 4.

Table 4. Normalized concentrations of the major elements obtained from X-ray microanalysis.

Elements	#1 (%wt)	#2 (%wt)	#3 (%wt)
Mg	2.6	2.9	1.8
Al	6.7	11.5	2.8
Si	21.8	38.5	12.1
S	0.4	0.4	3.7
Cl	1.2	<0.1	0.4
Ca	64.4	41.3	78.0
Fe	2.8	5.3	1.3

Hence, it was possible to determine a greater presence of silica, iron, sulfur, chlorine, potassium and sodium in Sample #2 than in Sample #1 and a meaningful lower measurement of the same elements in Sample #3, due to the use of a smaller amount of aggregate.

The high silica-based component for the aggregates of all samples was indicative of the excellent quality of mortars and a careful material selection, while the presence of aluminum and iron within the binder and not being related to the principal siliceous aggregates is a clue for the probable presence of clay, used as an additive. Therefore, despite appearing, at first, like aerial mortars due to the absence of crushed bricks or any kind of ceramic material and the abundance of calcium, the analyzed mortars could be ascribed to a typology having mixed aerial and hydraulic characteristics. In fact, hydraulic mortars can be distinguished for the development of silicates and aluminates coming from ceramics to form conglomerates or the use of marlstones, rich in carbonate minerals, clays and silt [14,31–36]. Moreover, in this case, the content of aluminum and iron was below the usual amount in the so-called hydraulic mortars. Moreover, the traces of sulfur and chlorine could be attributable respectively to gypsum and sodium chloride due to degradation for the sulfation process of the lime binder fraction and marine environment. Furthermore, the quality of the mortars regarding the silica and lime content was verified by means of structural analysis by using X-ray diffraction.

3.2. Structural Analysis

Through the X-ray diffractometric analysis, the mineral crystalline components of the mortars were investigated, highlighting the presence of quartz (SiO_2) and calcite ($CaCO_3$). A biphasic analysis of the crystalline components was carried out using the Rietveld method [37], allowing the detection of quartz and calcite for the three samples of mortars with some small impurities, ascribable to hematite (Fe_2O_3). The obtained percentages are reported in Table 5, which also shows the related percentages of silica and calcium resulting from microanalysis by using SEM-EDX. Regarding the render layer of the mortars, the results exhibit the careful selection of high-quality materials. In particular, the ratio between calcite and quartz in Sample #2 (0.90) corresponded with the one between Ca and Si (0.93), meaning nearly the totality of the silica and calcium amount is in the crystalline form. The different ratio between the silica and calcium content (2.9) and one of their mineral components (3.69) in Sample #1 is due to a lower quantity of quartz with respect to the %wt silica content, so as for Sample #3, which has completely different ratios (6.44 for the crystalline content against 1.63 for the total amount of calcium and silica). The undetected

presence of gypsum ($CaSO_4 \cdot 2(H_2O)$) and halite (NaCl) confirmed well-manufactured mortars made good preservation possible so that the small contaminants of sulfur and chlorine can be related to the ion absorption from the soil.

Table 5. Crystalline components in the mortars related to the percentages of silica and calcium.

Sample	Quartz (%wt)	Calcite (%wt)	Si (%wt)	Ca (%wt)
#1	21.3	78.7	21.8	64.4
#2	52.4	47.6	38.5	41.3
#3	38.0	62.0	12.1	78.0

3.3. Comparison with Local Materials

Different kinds of limestones from nearby quarries (Monteroni and Surbo) were analyzed by using XRD to verify a possible extraction from local sources. As shown in Table 6, Sample #6 and Sample #7, coming respectively from Monteroni and Surbo, had a similar percentage of calcite (67.4% for Sample #6 and 65.9% for Sample #7), but a different content of quartz (4.8% for Sample #6 and 1.1% for Sample #7). Moreover, Sample #6 had a considerable amount of periclase (MgO) (27.8%), while Sample #7 was characterized by wollastonite ($CaSiO_3$) (33%). Sample #8, taken from the Idume mouth (Frigole), consisted of a considerable quantity of seashell fragments, as proved by the presence of aragonite (41.7%), together with a small percentage of calcite (25.3%) and quartz (33%). Regarding the limestone source, the small content of magnesium revealed in the samples by means of SEM-EDX excluded the provenience from Monteroni. Similarly, the absence of wollastonite from the mortar samples did not make a correlation with Surbo possible. In fact, quicklime is produced by baking the raw materials based on calcium carbonate at a temperature of 850–900 °C, which is not sufficient for the degradation of wollastonite, considering it is stable up to 1150 °C [38]. Finally, the characteristic calcareous sand of Frigole was not compatible with the aggregates used in the mortars.

Table 6. Crystalline components in the Samples #6, #7 and #8.

Sample	Crystalline Components (%)
#6	Calcite (67.4%), Periclase (27.8%), Quartz (4.8%)
#7	Calcite (65.9%), Wollastonite (33%), Quartz (1.1%)
#8	Aragonite (41.7%), Quartz (33%), Calcite (25.3%)

Therefore, raw materials from distant sources were used for the lime, the aggregates and the presumed clay content. The effort of importing different materials, increasing the manufacturing costs, highlighted the important role of the abbey for which specific material selection was realized. In fact, the import of expensive materials has already been documented for this abbey by the extended use of the blue of lapis lazuli in the background of the wall paintings [1].

3.4. Radiocarbon Dating

Straw remains and vegetal fibers inside the mortars were exploited to determine the absolute dating of the frescoes. In fact, the dating of the fibers does not allow a direct chronology of the wall painting, as it does not refer to the plaster itself but the underlying layers. Anyway, it gives a useful timing threshold reference for the realization of the frescoes. While selecting through the stereomicroscope the fibers not strongly affected by the carbonation process of the mortars and the plasters, it was possible to identify among the fibers some glumes and culms belonging to the *genus triticum* of the family of graminaceous plants, compatible with the rural production that the area has had over the centuries.

For the two samples, conventional radiocarbon ages expressed in years in BP years were calibrated to calendar age using the Oxcal 4.4 software and the INTCAL20 curve based on atmospheric data (Figure 5).

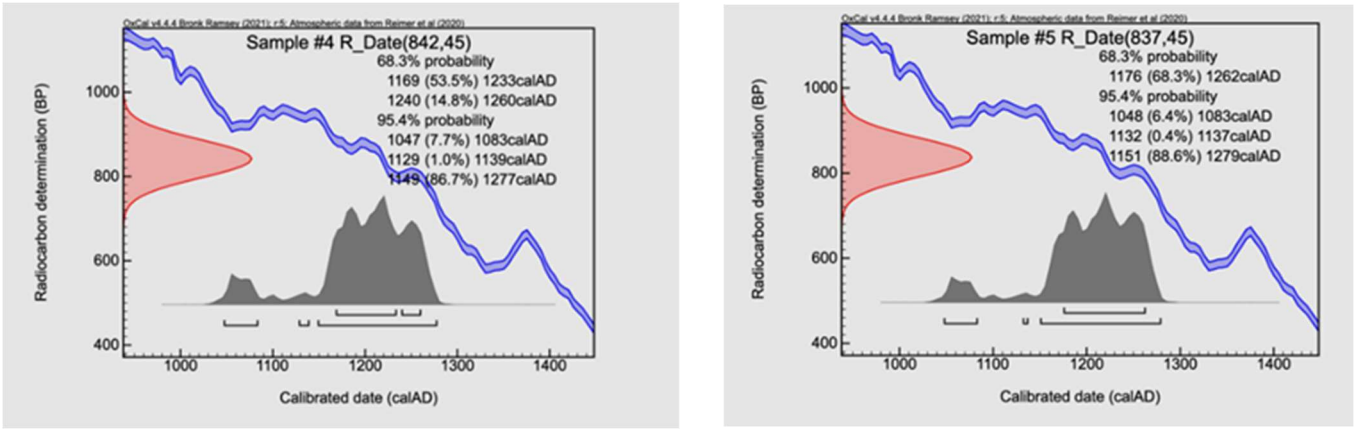

(**a**) (**b**)

Figure 5. Radiocarbon dating of Sample #4 (**a**) and of Sample #5 (**b**).

The Sample #4 and Sample #5 gave overlapping ages and they are dated between the end of the 12th century and the first half of the 13th century, scientifically confirming the stylistic dating previously carried out through careful historical-artistic research [3,4,12]. In Sample #4, although the fibers were taken next to the portion of the 14th-century frescoes, their dating is almost identical to the older frescoes on the left aisle. Moreover, this result shows that the portion of the wall taken into consideration was not affected by the collapse of the right masonry and that the 14th-century frescoes were realized starting from the plaster layer, using the previous *arriccio*.

4. Conclusions

Interdisciplinary analyses were performed to support the conservation and historical-artistic studies in the abbey of *Santa Maria di Cerrate* by means of characterization of materials for the cleaning, consolidation and integration actions. In particular, the three mortar samples, taken from significantly different points, had the purpose of suggesting the granulometry, and the most suitable materials fill the gaps in the masonry walls. Moreover, digital imaging processing allowed the identification of the aggregates-binder ratio from macro images and the presence of clay from micro images, expressing the perspective of an easy and non-destructive method.

SEM-EDX and XRD analyses applied to all the mortar samples showed a low percentage of impurities and a consistent siliceous component, denoting strong accuracy in the selection of the sand used for several building phases, while the small clay content highlighted the use of mixed aerial-hydraulic lime. The results were compared with local raw materials coming from the nearby quarries of Monteroni and Surbo and the sand of the Idume river mouth from Frigole, finding different and non-compatible characteristics.

Some vegetal remains, identified as a common byzantine practice, were sampled and dated, with radiocarbon dating by particle accelerator with AMS, between the end of the 12th century and the first half of the 13th century, also showing that one sample from the right aisle was not affected by the collapse of part of the same masonry. Therefore, as found in our previous studies regarding the pigments of the frescoes, mortars also highlighted the valuable role of the abbey through the careful selection of far and, consequently, expensive raw materials.

Author Contributions: Conceptualization, G.V., A.S., G.B., D.M., L.C., G.Q. and A.B.; methodology, G.V., A.S., G.B., D.M., L.C., G.Q. and A.B.; validation, G.V., A.S., G.B., D.M., L.C., G.Q. and A.B.; formal analysis, G.V., A.S., G.B., D.M., L.C., G.Q. and A.B.; investigation, G.V., A.S., G.B., D.M. and A.B.; resources, G.V., A.S., G.B., D.M., L.C., G.Q. and A.B.; data curation, G.V., A.S., G.B., D.M., L.C., G.Q. and A.B.; writing—original draft preparation, G.V., A.S., G.B., D.M., L.C., G.Q. and A.B.; writing—review and editing, G.V., A.S., G.B., D.M., L.C., G.Q. and A.B. All authors have read and agreed to the published version of the manuscript.

Funding: This research received no external funding.

Data Availability Statement: Data sharing not applicable.

Acknowledgments: The authors thank the FAI foundation, conservators and the Superintendence of Cultural Heritage for their collaboration.

Conflicts of Interest: The authors declare no conflict of interest.

References

1. Vasco, G.; Serra, A.; Manno, D.; Buccolieri, G.; Calcagnile, L.; Buccolieri, A. Investigations of Byzantine Wall Paintings in the Abbey of Santa Maria Di Cerrate (Italy) in View of Their Restoration. *Spectrochim. Acta Part A Mol. Biomol. Spectrosc.* **2020**, *239*, 118557. [CrossRef] [PubMed]
2. Conte, A.M.; Corda, L.; Esposito, D.; Giorgi, E. Characterization of Mortars from the Medieval Abbey of Cerrate (Southern Italy). *J. Archaeol. Sci. Rep.* **2017**, *12*, 463–479. [CrossRef]
3. Falla Castelfranchi, M. La Pittura Bizantina in Puglia (Secoli IX–XIV). In *Percorsi Bizantini nel Salento*; De Gruyter: Berlin, Germany, 2008; pp. 25–36.
4. Falla Castelfranchi, M. *Pittura Monumentale Bizantina in Puglia*, 1st ed.; Electa: Milano, Italy, 1991; ISBN 9788843537051.
5. Trono, A.; Fiore, N. (Eds.) *Travelling to the East on the Via Francigena: Through Art, Cultures and History*; Edizioni Esperidi: San Cesario di Lecce, Italy, 2012; ISBN 9788897895008.
6. Houben, H.; Vetere, B. (Eds.) *Pellegrinaggio e "Kulturtransfer" nel Medioevo Europeo: Atti del 1. Seminario di Studio dei Dottorati di Ricerca di Ambito Medievistico delle Università di Lecce e di Erlangen, Lecce, 2–3 Maggio 2003*; Congedo: Galatina, Italy, 2006; ISBN 9788880866671.
7. De Giorgi, C.T. *La Chiesa di S. Maria di Cerrate in Territorio di Lecce: Note Storiche Ed Archeologiche*; Tip. Lit. Luigi Lazzeretti e Figli: Lecce, Italy, 1889.
8. Barletta, R. *Santa Maria di Cerrate: La Storia Nascosta*; Edizioni del Grifo: Lecce, Italy, 2003.
9. Delli Ponti, G. *Cerrate e Il Suo Museo*; Amministrazione Provinciale di Lecce: Lecce, Italy, 1976.
10. Castromediano, S. *La Chiesa di S. Maria di Cerrate Nel Contado di Lecce: Ricerche*; Forgotten Books: London, UK, 2018; ISBN 9780483143425.
11. Pellegrino, T.; Luca, V.D. *Santa Maria a Cerrate: Antica Abbadia*; Capone Editore: Lecce, Italy, 2004; ISBN 9788883490934.
12. De Giorgi, M. *Il Transito della Vergine: Testi e Immagini dall'Oriente al Mezzogiorno Medievale*; Fondazione CISAM: Spoleto, Italy, 2016.
13. Miriello, D.; Crisci, G.M. Image Analysis and Flatbed Scanners. A Visual Procedure in Order to Study the Macro-Porosity of the Archaeological and Historical Mortars. *J. Cult. Herit.* **2006**, *7*, 186–192. [CrossRef]
14. Moropoulou, A.; Bakolas, A.; Bisbikou, K. Investigation of the Technology of Historic Mortars. *J. Cult. Herit.* **2000**, *1*, 45–58. [CrossRef]
15. Moropoulou, A.; Bakolas, A.; Bisbikou, K. Physico-Chemical Adhesion and Cohesion Bonds in Joint Mortars Imparting Durability to the Historic Structures. *Constr. Build. Mater.* **2000**, *14*, 35–46. [CrossRef]
16. Rampazzi, L.; Colombini, M.P.; Conti, C.; Corti, C.; Lluveras-Tenorio, A.; Sansonetti, A.; Zanaboni, M. Technology of Medieval Mortars: An Investigation into the Use of Organic Additives. *Archaeometry* **2016**, *58*, 115–130. [CrossRef]
17. Akcay, C.; Sayin, B.; Yildizlar, B. The Conservation and Repair of Historical Masonry Ruins Based on Laboratory Analyses. *Constr. Build. Mater.* **2017**, *132*, 383–394. [CrossRef]
18. Miriello, D.; Lezzerini, M.; Chiaravalloti, F.; Bloise, A.; Apollaro, C.; Crisci, G.M. Replicating the Chemical Composition of the Binder for Restoration of Historic Mortars as an Optimization Problem. *Comput. Concr.* **2013**, *12*, 553–563. [CrossRef]
19. Sanjurjo-Sánchez, J. An Overview of the Use of Absolute Dating Techniques in Ancient Construction Materials. *Geosciences* **2016**, *6*, 22. [CrossRef]
20. Hajdas, I.; Ascough, P.; Garnett, M.H.; Fallon, S.J.; Pearson, C.L.; Quarta, G.; Spalding, K.L.; Yamaguchi, H.; Yoneda, M. Radiocarbon Dating. *Nat. Rev. Methods Prim.* **2021**, *1*, 62. [CrossRef]
21. Sanjurjo-Sánchez, J. Dating Historical Buildings: An Update on the Possibilities of Absolute Dating Methods. *Int. J. Archit. Herit.* **2016**, *10*, 620–635. [CrossRef]
22. Abramoff, M.D.; Magalhães, P.J.; Ram, S.J. Image Processing with ImageJ. *Biophotonics Int.* **2004**, *11*, 36–42.
23. D'Elia, M.; Calcagnile, L.; Quarta, G.; Sanapo, C.; Laudisa, M.; Toma, U.; Rizzo, A. Sample Preparation and Blank Values at the AMS Radiocarbon Facility of the University of Lecce. *Nucl. Instrum. Methods Phys. Res. Sect. B Beam Interact. Mater. At.* **2004**, *223–224*, 278–283. [CrossRef]

24. Taglieri, G.; Rigaglia, D.; Arrizza, L.; Daniele, V.; Macera, L.; Rosatelli, G.; Romè, V.; Musolino, G. Microanalytical Investigations on a Byzantine Fresco of the Dormitio Virginis from Sicily. *J. Cult. Herit.* **2019**, *40*, 155–162. [CrossRef]
25. Miriello, D.; Antonelli, F.; Apollaro, C.; Bloise, A.; Bruno, N.; Catalano, M.; Columbu, S.; Crisci, G.M.; De Luca, R.; Lezzerini, M.; et al. A Petro-Chemical Study of Ancient Mortars from the Archaeological Site of Kyme (Turkey). *Period. Mineral.* **2015**, *84*, 497–517. [CrossRef]
26. Singh, M.; Vinodh Kumar, S.; Waghmare, S.A. Characterization of 6–11th Century A.D Decorative Lime Plasters of Rock Cut Caves of Ellora. *Constr. Build. Mater.* **2015**, *98*, 156–170. [CrossRef]
27. Sansò, P.; Margiotta, S.; Mastronuzzi, G.; Vitale, A. The Geological Heritage of Salento Leccese Area (Apulia, Southern Italy). *Geoheritage* **2015**, *7*, 85–101. [CrossRef]
28. Bakolas, A.; Biscontin, G.; Moropoulou, A.; Zendri, E. Characterization of Structural Byzantine Mortars by Thermogravimetric Analysis. *Thermochim. Acta* **1998**, *321*, 151–160. [CrossRef]
29. Moropoulou, A.; Labropoulos, K.; Moundoulas, P.; Bakolas, A. The Contribution of Historic Mortars on the Earthquake Resistance of Byzantine Monuments. In *Measuring, Monitoring and Modeling Concrete Properties*; Konsta-Gdoutos, M.S., Ed.; Springer: Dordrecht, The Netherlands, 2006; pp. 643–652.
30. Moropoulou, A.; Cakmak, A.S.; Lohvyn, N. Earthquake Resistant Construction Techniques and Materials on Byzantine Monuments in Kiev. *Soil Dyn. Earthq. Eng.* **2000**, *19*, 603–615. [CrossRef]
31. Pintér, F.; Weber, J.; Bajnóczi, B.; Tóth, T. Brick-Lime Mortars and Plasters of a Sixteenth Century Ottoman Bath from Budapest, Hungary. In Proceedings of the 37th International Symposium on Archaeometry, Siena, Italy, 13–16 May 2008; Turbanti-Memmi, I., Ed.; Springer: Berlin/Heidelberg, Germany, 2008. [CrossRef]
32. Pintér, F.; Vidovszky, I.; Weber, J.; Bayer, K. Mineralogical and microstructural characteristics of historic Roman cement renders from Budapest, Hungary. *J. Cult. Herit.* **2014**, *15*, 219–226. [CrossRef]
33. Franquelo, M.; Robador, M.; Ramirez-Valle, V.; Durán, A.; Jimenéz de Haro, M.; Pérez-Rodruigez, J. Roman ceramics of hydraulic mortars used to build the Mithraeum house of Mérida (Spain). *J. Therm. Anal. Calorim.* **2008**, *92*, 331–335. [CrossRef]
34. Keppert, K.; Kobera, L.; Scheinherrová, L.; Doleželová, M.; Brus, J.; Černý, R. Kinetics of pozzolanic reaction and carbonation in ceramic-lime system: Thermogravimetry and solid-state NMR spectroscopy study. *J. Build. Eng.* **2020**, *32*, 101729. [CrossRef]
35. Arizzi, A.; Cultrone, G. Mortars and plasters—How to characterse hydraulic mortars. *Archaeol. Anthropol. Sci.* **2021**, *13*, 144. [CrossRef]
36. Michalska, D.; Czernik, J. Carbonates in leaching reactions in context of 14C dating. *Nucl. Instrum. Methods Phys. Res. Sect. B Beam Interact. Mater. At.* **2015**, *361*, 431–439. [CrossRef]
37. Rietveld, H.M. The Rietveld Method. *Phys. Scr.* **2014**, *89*, 098002. [CrossRef]
38. Sokolova, T.S.; Dorogokupets, P.I. Equations of State of Ca-Silicates and Phase Diagram of the $CaSiO_3$ System under Upper Mantle Conditions. *Minerals* **2021**, *11*, 322. [CrossRef]